THE JOURNAL OF COMPARATIVE NEUROLOGY 256:88-103 (1987)

Neural Inputs Into the Temporopolar Cortex of the Rhesus Monkey

M.A. MORÁN, E.J. MUFSON, AND M.-M. MESULAM
Bullard and Denny-Brown Laboratories, Division of Neuroscience and Behavioral Neurology of the Harvard Neurology Department and the Charles A. Dana Research Institute of Beth Israel Hospital, Boston, Massachusetts 02215

ABSTRACT

Temporopolar cortex (TP) can be subdivided into agranular, dysgranular, and granular components. The telencephalic input into the temporopolar cortex arises from the orbitofrontal and medial frontal regions, modality-specific visual and auditory association areas, paralimbic regions, the piriform olfactory cortex, the hippocampus, the amygdala, the claustrum, and the basal forebrain.

Afferents from limbic and paralimbic regions are directed mostly to the agranular and dysgranular sectors of the temporal pole, whereas afferents from isocortical association areas are distributed predominantly within the granular sector.

The temporopolar cortex provides a site for the potential convergence of sensory and limbic inputs. Auditory inputs predominate in the dorsolateral part of the temporopolar cortex whereas visual inputs become prominent only in the ventral portions of this region. Olfactory inputs are directed mostly to the medial parts of the temporal pole. These medial parts also receive more extensive projections from the amygdaloid nuclei.

Key words: horseradish peroxidase, paralimbic, architectonics, connectivity, sensory-limbic interaction

The temporopolar cortex (TP) is one of the major paralimbic (mesocortical) components of the primate brain. It provides a zone of cytoarchitectonic transition interposed between the medially situated olfactory allocortex and the granular association cortex of the lateral temporal lobe.

Investigations employing strychnine neuronography demonstrated that TP is reciprocally interconnected with the posterior orbital cortex, the anterior insula, the anterior part of the fusiform gyrus, the amygdaloid complex, the entorhinal cortex and the anterior hippocampus (Pribram et al., '50; Pribram and MacLean, '53). Subsequent studies with anterograde degeneration methods reported efferent projections from TP to orbitofrontal regions, temporal cortex (areas TA, TE, and TH of von Bonin and Bailey, '47), the subcallosal part of the anterior cingulate cortex, the prorhinal and entorhinal cortices, the amygdaloid complex, the olfactory tubercle, and the caudal hippocampus (Pandya and Kuypers, '69; Jones and Powell, '70; Van Hoesen et al., '72, '76; Van Hoesen and Pandya, '75a,b; Herzog and Van Hoesen '76; Turner et al., '80).

Axonal transport methods have also been employed to trace the connections of TP. These studies have shown TP projections to the insula, the parasubiculum, the striatum, and the nucleus basalis (Van Hoesen et al., '79, '81; Mufson and Mesulam, '82; Mesulam and Mufson, '84). Other projections into TP have been described from the subiculum (Rosene and Van Hoesen, '77), amygdaloid nuclei (Amaral and Price, '84), the insula (Mufson and Mesulam, '82), the superior temporal region (Galaburda and Pandya, '83), the thalamus (Gower '81; Markowitsch et al., '85), the entorhinal cortex (Kosel et al., '82), and the nucleus basalis (Mesulam et al., '83).

The present study, based on horeradish peroxidase (HRP) and tritiated amino acid (TAA) injections, aims to consolidate and supplement existing information on the afferent projections to area TP. This investigation is part of an ongoing evaluation of the connectivity of the orbito-insulo-temporopolar component of paralimbic cortex (Mesulam and Mufson, '82a,b; '85; Mufson and Mesulam, '82, 84). Recently, Markowitsch et al., ('85) reported a comprehensive account of afferents to lateral TP. Our observations are in

Accepted August 7, 1986.

Address reprint requests to M. Mesulam, Department of Neurology, K-416, Beth Israel Hospital, Boston, MA 02215.

agreement with their conclusions and provide additional information about the connections of medial TP.

MATERIALS AND METHODS

In 15 male adolescent and adult rhesus monkeys *(Macaca mulatta)* either HRP or a mixture of tritiated amino acids (TAA) was injected into selected cortical areas under visual guidance. Two additional macaque specimens were embedded in celloidin, cut serially at 35-μm thickness in the coronal plane, and stained with cresyl violet for a more extensive analysis of the pertinent cytoarchitectonic detail.

Surgery and tracer injection

Surgery was performed in aseptic conditions under sodium pentobarbital anesthesia (35 mg/kg). Craniotomy was preceded by an intravenous infusion of 50 ml of 25% mannitol (Invenenx, Ohio). This provided a reduction in the volume of intracranial contents and facilitated the subsequent exposure of the desired cortical area. After reflection of the dura, the tracer was delivered with a 5-μl Hamilton microsyringe mounted on a micromanipulator attached to a Kopf stereotoxic carrier. The needle was lowered to the desired target site under microscopic guidance and the tracer was delivered 1.0–1.5 mm below the pial surface at each of two or three adjacent sites separated by 1–2 mm. The delivery of the tracer started 3–5 minutes after needle penetration and lasted approximately 5–10 minutes. The needle was withdrawn 5 minutes after the termination of the injection.

HRP histochemistry

A volume of 0.02–0.05 μl of HRP was injected into TP in four animals. The tracer was 20% (aqueous) free HRP (Miles Laboratories, Kankakee, IL) in one animal and 10% (aqueous) HRP conjugated to wheat germ agglutinin (WGA) in the other three (Mesulam, '82). After 48 hours the monkeys were reanesthetized and perfused transcardially according to procedure II of Rosene and Mesulam ('78). The brain was removed from the skull; the hemispheres were separated and photographed. The injected hemisphere was transferred onto a freezing microtome, cut in the coronal plane at 40-μm thickness, and collected in 0.1 M phosphate buffer (pH 7.4). Every tenth section was treated for the visualization of HRP with the chromogen tetramethylbenzidine (TMB) according to the procedures described elsewhere (Mesulam, '78, '82; Mesulam et al., '80). Neutral red was used as a counterstain in these sections. Additional adjacent sections were stained with thionin.

TAA autoradiography

In 11 animals, selected cortical regions were injected with an amino acid mixture prepared by desiccating equal parts (in μCi) of radioactive proline (L-2,2,4,5,-^{3}H (N), 100 Ci/mmol), leucine (L-3,4,5-^{3}H (N), 110 Ci/mmol), lysine (L-4,5-^{3}H (N), 60–80 Ci/mmol), and a tritiated amino acids mixture (New England Nuclear, Boston, MA) and then reconstituting this to a concentration of 50–75 μCi/μl with physiological saline. The volume of each injection varied from 0.1 to 0.3 μl. After 7–15 survival days, the animals were perfused with physiological saline followed by 10% formalin. The hemisphere was embedded in paraffin, cut on a rotatory microtome in the coronal plane at 10-μm thickness, and processed according to the procedure of Cowan et al. ('72). The development period was 14–54 weeks. All the sections were counterstained with thionin.

Data analysis

The injection site and the distribution of transported label were traced onto graph paper with an X-Y plotter (Hewlett Packard, 7044A) that was electronically coupled to the stage of a Nikon microscope. In the HRP experiments, sections were examined microscopically under brightfield illumination for the detection of labeled perikarya and the determination of architectonic boundaries. Although all sections prepared for HRP histochemistry were evaluated, only every other section (separated approximately by 800 μm) was charted. Additional matched sections were studied through the thalamus in order to observe labeling in the closely spaced thalamic nuclei. The center of the HRP injection site was defined as an area containing such intense precipitation of reaction product that neither cells nor axons were individually distinguishable. The less densely labeled region surrounding this center was considered the halo of the injection site. The problems inherent in the histochemical demonstration of an "injection site" have been discussed previously (Mesulam, '82). In this study, we interpreted the results conservatively by assuming that the center and halo had both participated in the uptake and retrograde transport of the tracer. Labeled neurons in cortex and amygdaloid nuclei were counted in regularly spaced sections that spanned the whole brain. Positive perikarya within a 0.5-mm radius from the halo of the injection site were excluded to avoid the possibility of counting cells labeled through passive diffusion of the injected tracer. Sections examined for the autoradiographic distribution of labeled grains were first evaluated under darkfield illumination and subsequently under brightfield illumination for the determination of architectonic boundaries. The TAA injection site was defined as the region around the needle track where label was uniformly intense over cell bodies as well as over the neuropil. Other regions where the autoradiographic labeling was substantially and consistently above the background level were considered to receive a projection from the injection site.

RESULTS

Temporopolar architectonics

The temporopolar cortex (TP) covers the rostral tip of the temporal lobe and extends to the limen insula medially and to the rostral tip of the superior temporal sulcus laterally. This cortex has been designated as area 38 by Brodmann ('09), TG by von Bonin and Bailey ('47), Ts1, Ts2, and Pro by Pandya and Sanides ('73), and TP by Mesulam and Mufson ('82a).

Analysis of sections stained for Nissl substance confirmed earlier observations (Gower and Mesulam, '82; Mesulam and Mufson, '82a). The overall plan of organization indicates a concentric arrangement of increasingly more differentiated agranular, dysgranular, and granular sectors arranged around an allocortical core provided by the piriform portion of the olfactory cortex (POC) (Fig. 1). The agranular-periallocortical sector (TPa-p) underlies POC and is also directly contiguous with it. The TPa-p sector covers part of the free medial surface of the temporal pole and extends caudally beyond the limen insula until the emergence of the amygdala. The TPa-p sector has a relatively simple organization consisting of an outer, an intermediate, and an inner lamina. The outer lamina contains clusters of hyperchromic neurons that in places appear continuous with the cells of POC. In Nissl preparations, the inner

Abbreviations

A	Arcuate sulcus
AA	Anterior amygdaloid area[2]
a10,11, 12,13, 14	Cortical areas[1]
ac	Anterior commissure
amg	Amygdala
B	Basal amygdaloid nucleus[2]
BA	Basal accessory amygdaloid nucleus[2]
Bl	Lateral division of the basal amygdaloid nucleus[2]
Bm	Medial division of the basal amygdaloid nucleus[2]
C	Central sulcus
cd	Caudate
Cdc	Centralis densocellularis nucleus[4]
Ce	Central amygdaloid nucleus[2]
CF	Calcarine fissure
CG	Cingulate sulcus
Ch4a	Anterior division of the cholinergic cell group 4[3]
Ch4i	Intermediate division of the cholinergic cell group 4[3]
Ch4p	Posterior division of the cholinergic cell group 4[3]
CL	Claustrum
CM	Centromedian nucleus[4]
Co	Cortical amygdaloid nucleus[2]
CTA	Cortical amygdaloid transition area[2]
ENT	Entorhinal cortex
H	Hippocampus
HF	Hippocampal fissure
hy	Hypothalamus
Ia-p	Insula, agranular periallocortical[5]
ic	Internal capsule
Idg	Insula, dysgranular[5]
IO	Inferior occipital sulcus
INS	Insula
IP	Intraparietal sulcus
L	Lateral amygdaloid nucleus[2]
LF	Lateral sulcus
Lim	Limitans nucleus[4]
LN	Lunate sulcus
LO	Lateral orbitofrontal sulcus
LP	Lateral posterior nucleus[4]
M	Medial amygdaloid nucleus[2]
MD	Medial dorsal nucleus[4]
MDdc	Medial dorsal nucleus, densocellular division[4]
MGmc	Medial geniculate nucleus, magnocellular division[4]
MGpc	Medial geniculate nucleus, parvicellular division[4]
nb	Nucleus basalis
OFa-p	Orbitofrontal cortex, agranular periallocortical[5]
OFdg	Orbitofrontal cortex, dysgranular[5]
OFg	Orbitofrontal cortex, granular[5]
OT	Occipitotemporal sulcus
ot	Optic tract
P	Principal sulcus
Pa	Paraventricular nucleus[4]
Pac	Caudal paraventricular nucleus[4]
PaS	Parasubiculum
PI	Parainsula
Pf	Parafascicular nucleus[4]
PO (FL)	Paraolfactory cortex
POC	Piriform primary of olfactory cortex
Pr	Prorhinal cortex
pt	Putamen
Pul_i	Inferior division of the pulvinar nucleus[4]
Pul_l	Lateral division of the pulvinar nucleus[4]
Pul_m	Medial division of the pulvinar nucleus[4]
R	Rhinal sulcus
Re	Reuniens nucleus[4]
Ro	Rostral sulcus
SG	Supragenicular nucleus[4]
ST	Superior temporal sulcus
TA	Superior temporal cortex[6]
TE	Inferior temporal cortex[6]
TE_m	Inferior temporal cortex, medial part
TF	Parahippocampal cortex[6]
Tga	Anterior tegmental nucleus[4]
TH	Parahippocampal cortex[6]
thi	Habenulointerpeduncular tract
TMA	Temporal medial anterior sulcus
to	Olfactory tract
TP	Temporopolar cortex
TPa-p	Temporopolar cortex, agranular periallocortical[5]
TPdg	Temporopolar cortex, dysgranular[5]
TPdg-TE_m	Junction of TPdg with TE_m
TPg	Temporopolar cortex, granular[5]
V	Ventricle
VA	Ventral anterior nucleus[4]
VLo	Oral division of the ventral lateral nucleus[4]
VLc	Caudal division of the ventral lateral nucleus[4]
VPLc	Caudal division of the ventral posterior lateral nucleus[4]
VPLo	Oral division of the ventral posterior lateral nucleus[4]

[1]According to Walker ('40).

[2]According to Lauer ('45) and Herzog and Van Hoesen ('76).

[3]According to Mesulam et al. ('83).

[4]According to Olszewski ('52).

[5]According to Mesulam and Mufson ('82a).

[6]According to von Bonin and Bailey ('47).

lamina stains darker than the intermediate lamina. A major defining property of TPa-p is the virtual absence of granule cells. Evidence of increasing differentiation can be seen in the cortex that surrounds TPa-p. This differentiation proceeds along several dimensions: the appearance of a granular layer 4, the separation of the infragranular layers into L5 and L6, the sublamination of layer 3, and eventually the appearance of a granular layer 2. The cortical area where this differentiation occurs is designated as the dysgranular part of TP (TPdg). At the culmination of this process of differentiation, the cortex has a six-layered, well-granularized structure that is consistent with the designation of isocortex. This granular component of TP is designated as TPg. Thus, TP, which is a paralimbic region, contains both nonisocortical (TPa-p and TPdg) sectors as well as an isocortial component (TPg). On coronal sections, it is possible to identify both dorsal and ventral TPdg sectors. From these dysgranular sectors, increasing differentiation proceeds lateralward toward the TPg cortex of the lateral temporal pole. The tip of the temporal pole is covered by TPdg. On the floor of the sylvian fossa, and at a point caudal to the limen insula, TPdg is continuous with the parainsular cortex (PI), which can be considered a caudal extension of TPdg (Mesulam and Mufson, '82a).

HRP injections

Of the four animals with HRP injections, three representative cases will be described in detail.

Case A. This injection site was in the anterolateral portion of dorsal TP (Fig. 2A). It was centered mainly in the granular sector of TP (TPg) (Fig. 3, sections 6,7). Rostrally, the injection site spread to the anterior dysgranular portion of TP (TPdg) (Fig. 3, section 5). The HRP reaction product did not extend to TPa-p or POC. The needle tract did not penetrate the white matter.

Case B. This injection site was primarily focused in the anteromedial portion of dorsal TPdg (Figs. 2B, 4, sections 7,8). The halo of HRP reaction product extended caudally to

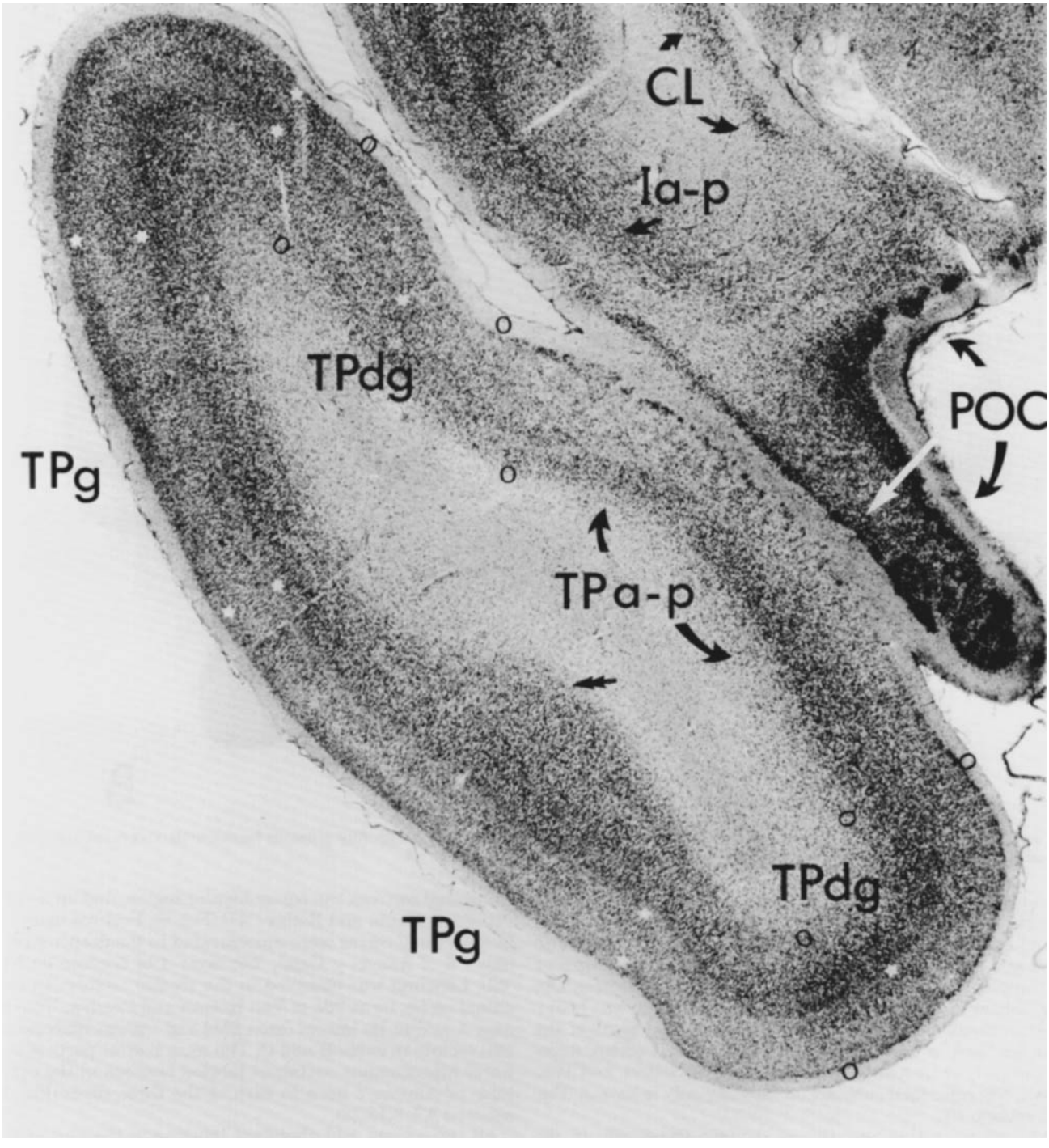

Fig. 1. Photomicrograph of TP showing its cytoarchitectonic boundaries (open circles). White stars indicate the position of layer 4 and layer 2 granules. The prepiriform olfactory allocortex (POC) overlies the agranular TPa-p. TPa-p is surrounded by a peri-isocortical region (TPdg), which is, in turn, flanked by an isocortical zone (TPg). The double arrowhead points to the rostral inception of the superior temporal sulcus. ×10.

the deeper layers of TPa-p (Fig. 4, section 9). There was no spread of injectate to TPg or POC.

Case C. The injection site was centered in the most anterior portion of ventral TPdg (Fig. 5, section 7). A halo of HRP reaction product extended to TPa-p, probably to ventral TPg and to the underlying white matter (Fig. 5, sections 8,9). As in cases A and B, there was no spread of injectate to POC.

Perikaryal labeling

Cortical labeling was remarkably selective. Almost all labeled neurons were found in the anterior half of the temporal lobe, in orbitofrontal cortex, and in the medial frontal region (Figs. 3–5).

Lateral, anterior, and inferior temporal lobe. In each case, numerous HRP-positive neurons were found in the TP

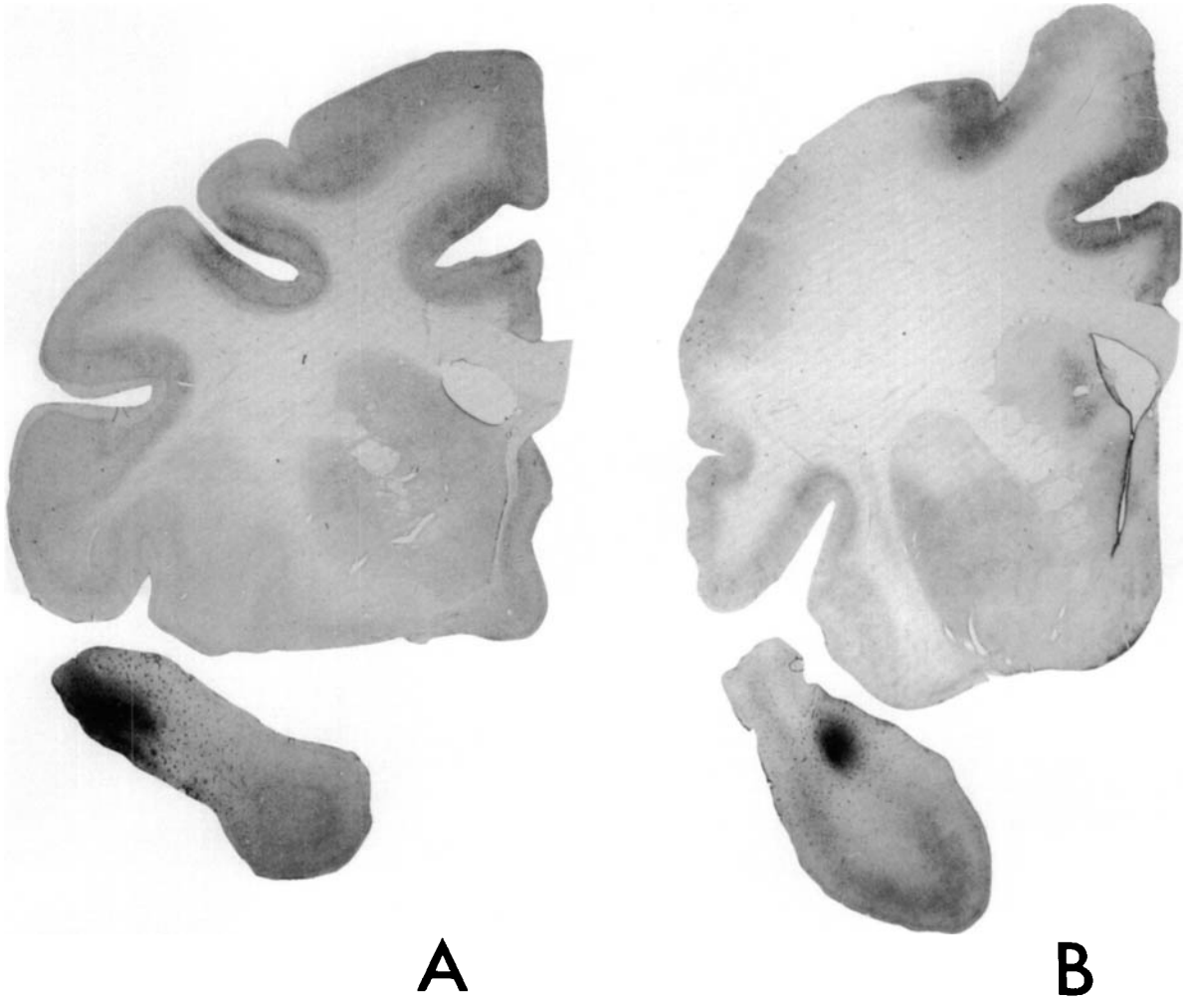

Fig. 2. Photomicrographs of coronal sections through the injection site of case A, in which HRP was centered in the anterolateral portion of dorsal TP, and case B, with HRP primarily focused in the anteromedial portion of dorsal TPdg. ×4.

sectors adjacent to the injection site and in the anterior part of the superior temporal gyrus (area TA of von Bonin and Bailey, '47) (Figs. 3–5). Labeled neurons were also present in the rostral half of the upper bank of the superior temporal sulcus (topographically corresponding to area TAa of Seltzer and Pandya, '78). This sulcal labeling was heaviest in cases A and C (Figs. 3,5). More medial parts of the upper bank of the superior temporal sulcus cortex (topograpically corresponding to area TPO of Seltzer and Pandya, '78) contained substantial labeling only in case A (Fig. 3, section 10).

Labeling in the supratemporal plane (especially in the parainsular (PI) region) existed in all three cases but was most prominent in case A (Fig.4, sections 10–12). According to the nomenclature of Pandya and Sanides ('73), the sites of supratemporal labeling included areas Pro, Ts2, Ts3, paI, and paAr. Labeling in the lower bank of the superior temporal sulcus occurred only in case C, in which the injection site was focused in the ventral portion of TPdg (Fig. 5, section 12). Inferotemporal labeling (areas TE and TEm) was present in cases A and C but was much heavier in the latter (Fig. 5 sections 10, 11).

Medial temporal lobe, hippocampus, and amygdala. In all cases, consistent labeling was seen in the prorhinal and entorhinal cortices, the parasubicular region, and areas TF-TH of von Bonin and Bailey ('47) (Fig. 6). Positive neurons in entorhinal cortex were concentrated in the deeper strata (layer 5 of Ramón y Cajal, '55; layer 4 of Lorente de Nó, '33). Labeling was observed in the medial sectors of entorhinal cortex (area 28a of Van Hoesen and Pandya, '75a) in case A and in its lateral (area 28b) and intermediate (area 28i) sectors in cases B and C. The most rostral parts of the uncal hippocampus contained labeled neurons in the pyramids of Ammon's horn in each of the three cases (Fig. 6, sections 3,7, 8,12,13).

All three cases had abundant labeling in the amygdala. This was much more prominent in cases B and C when compared to case A (Fig. 6, sections 1,6,11). In case A, labeled perikarya were restricted to parts of the lateral and accessory basal nuclei (Fig. 6, sections 1,2). In contrast, in cases B and C HRP-positive neurons had a more widespread distribution within the lateral nucleus and were also found within the accessory basal, lateral basal, medial basal, cortical, central, and medial nuclei as well as in the anterior amygdaloid region and in the cortical amygdaloid transition area (Fig. 6, sections 6,7,11,12).

Frontal cortex and the cingulate complex. In all three cases, positive neurons were found in the orbitofrontal re-

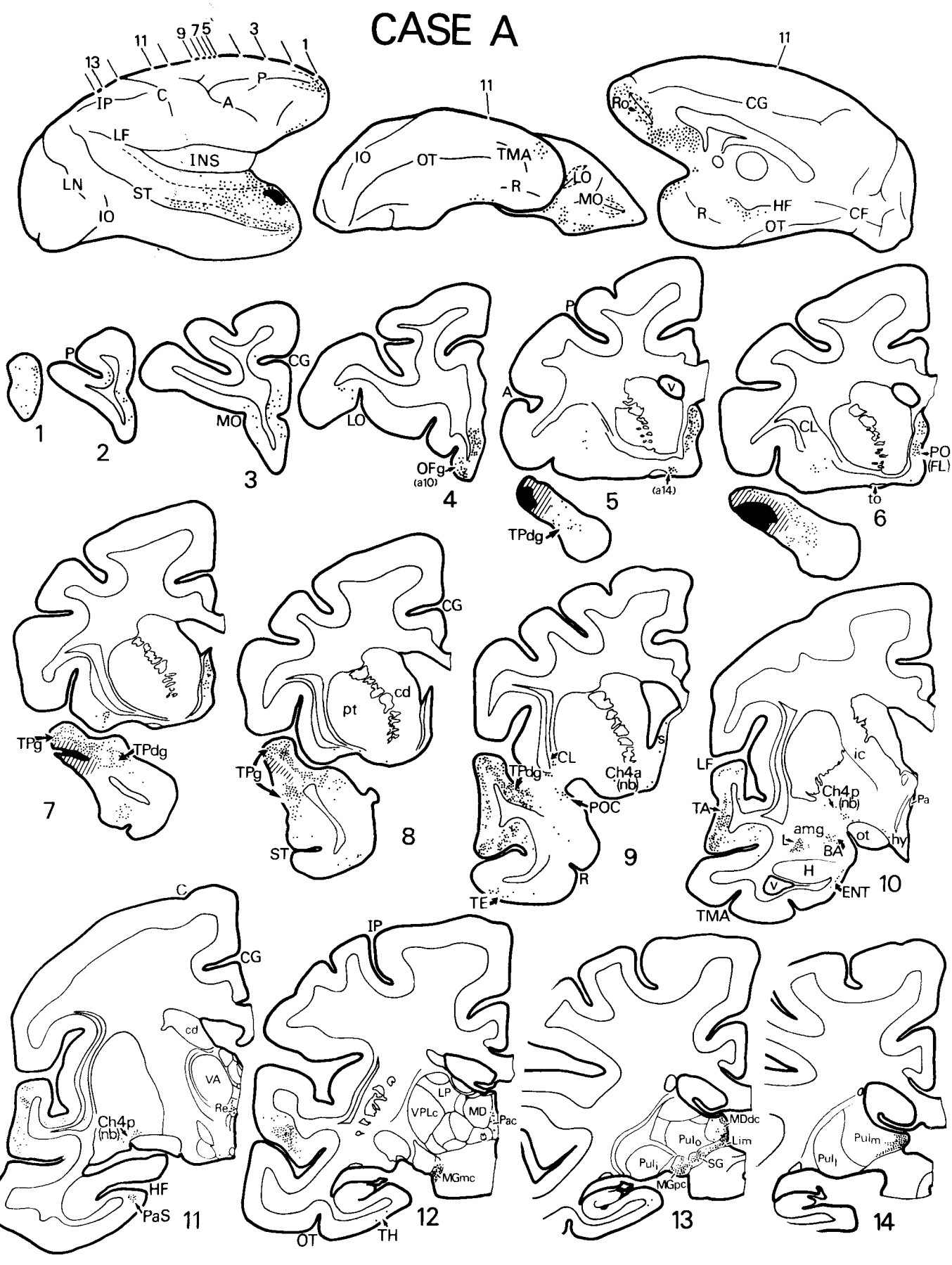

Fig. 3. Case A with HRP injected into the anterolateral portion of dorsal TP. The injection site is shown as solid black and the halo of reaction product is shown with slanted lines. The areas containing labeled neurons are indicated with black dots. At the top of the figure the lateral, ventral, and medial surfaces of the macaque brain are illustrated from left to right. The areas between dotted and solid lines represent cortex along the banks of sulci. The lateral (sylvian) fissure has been opened in the lateral view to show the insula. The region between the ventral boundary of the insula and the dotted line below it contains the parainsular belt and the supratemporal plane.

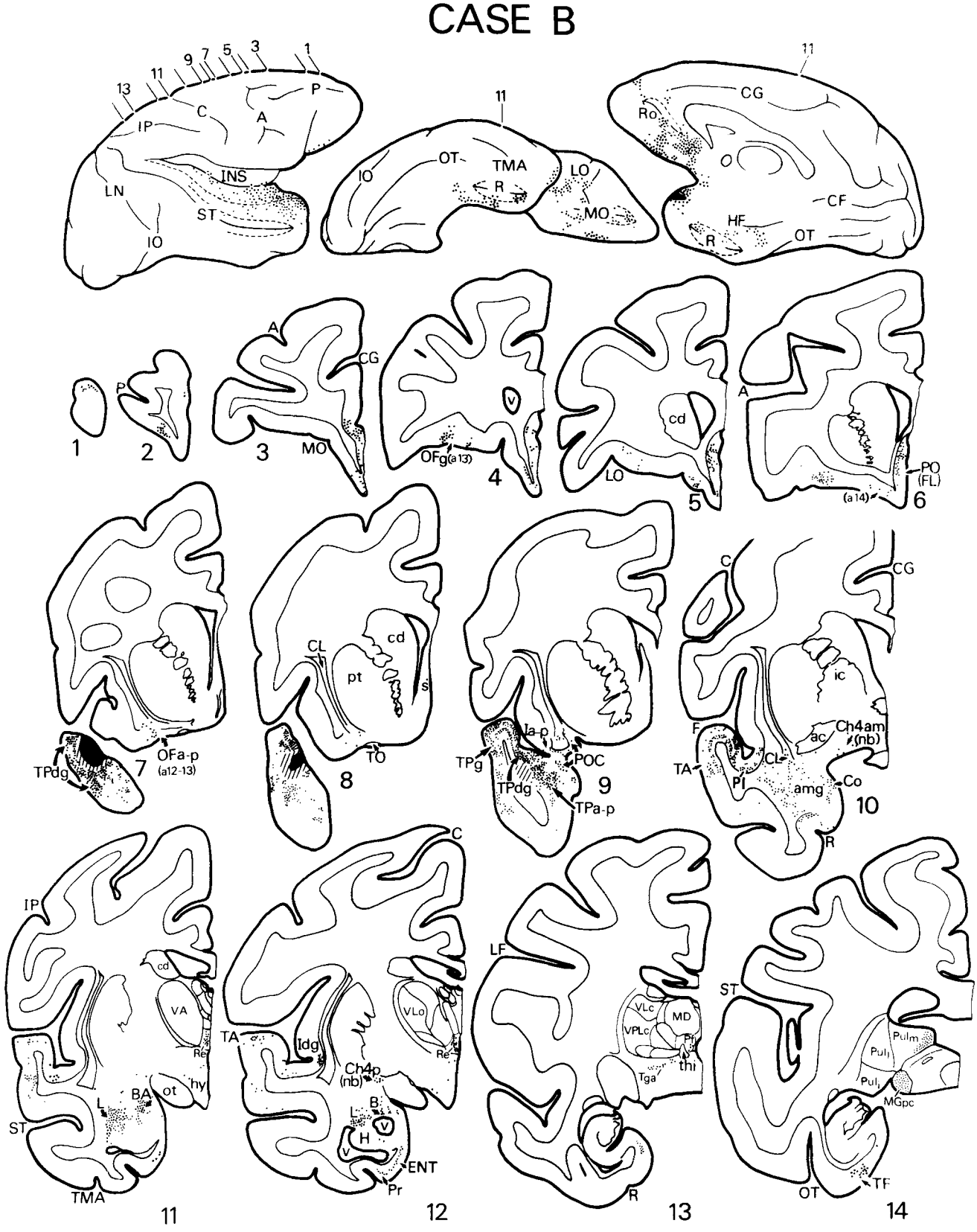

Fig. 4. Case B with the HRP injection primarily focused in the anteromedial portion of dorsal TPdg. The injection site is shown as solid black and the halo of reaction product is shown with slanted lines. The areas containing labeled neurons are indicated with black dots. At the top of the figure the lateral, ventral, and medial surfaces of the macaque brain are illustrated from left to right. The areas between dotted and solid lines represent cortex along the banks of sulci. The lateral (sylvian) fissure has been opened in the lateral view to show the insula. The region between the ventral boundary of the insula and the dotted line below it contains the parainsular belt and the supratemporal plane.

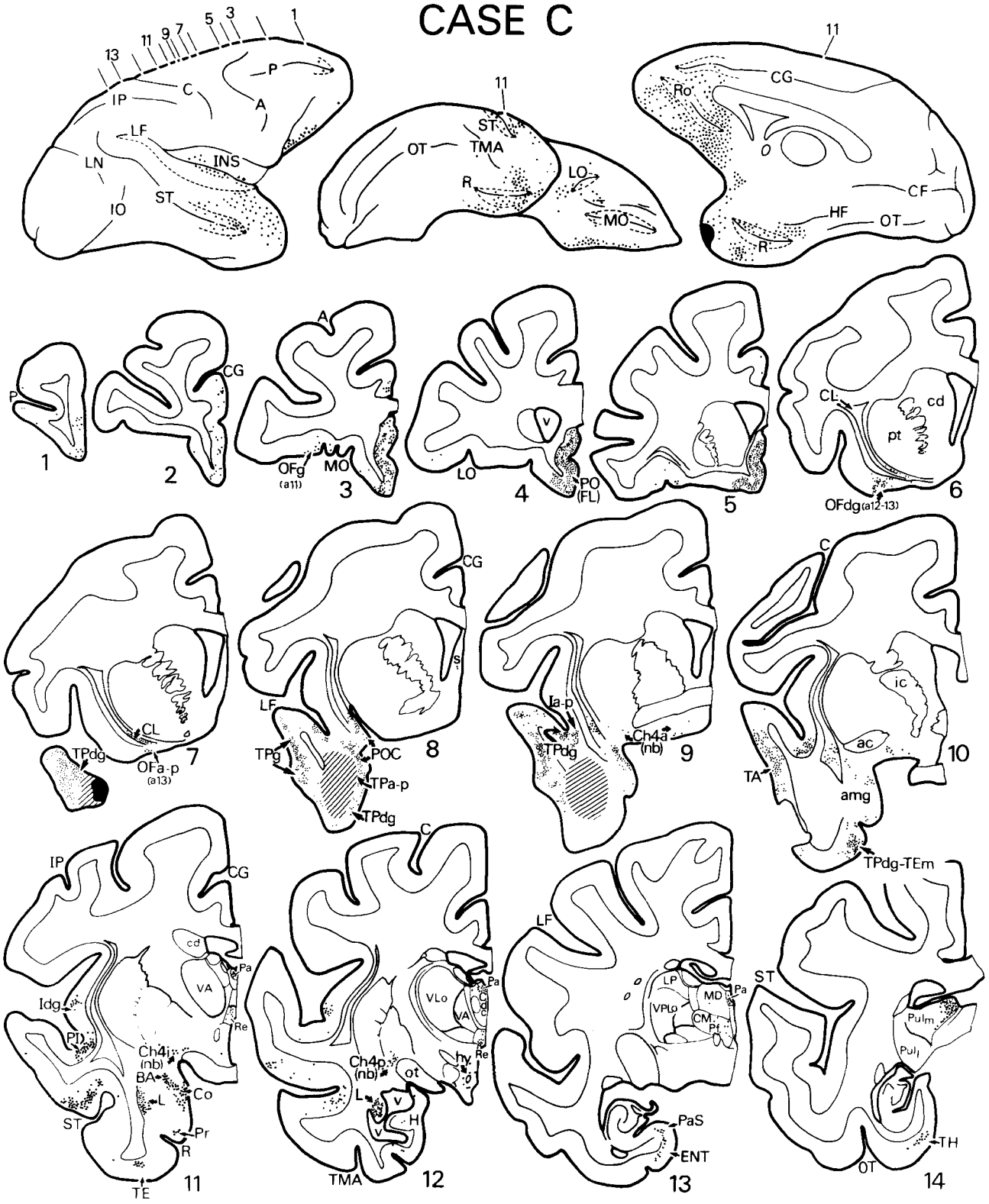

Fig. 5. Case C with the injection site centered in the most anterior portion of ventral TPdg. Solid black represents the injection site and slanted lines the halo of reaction product. The areas containing labeled neurons are indicated with black dots. At the top of the figure the lateral, ventral, and medial surfaces of the macaque brain are illustrated from left to right. The areas between dotted and solid lines represent cortex along the banks of sulci. The lateral (sylvian) fissure has been opened in the lateral view to show the insula. The region between the ventral boundary of the insula and the dotted line below it contains the parainsular belt and the supratemporal plane.

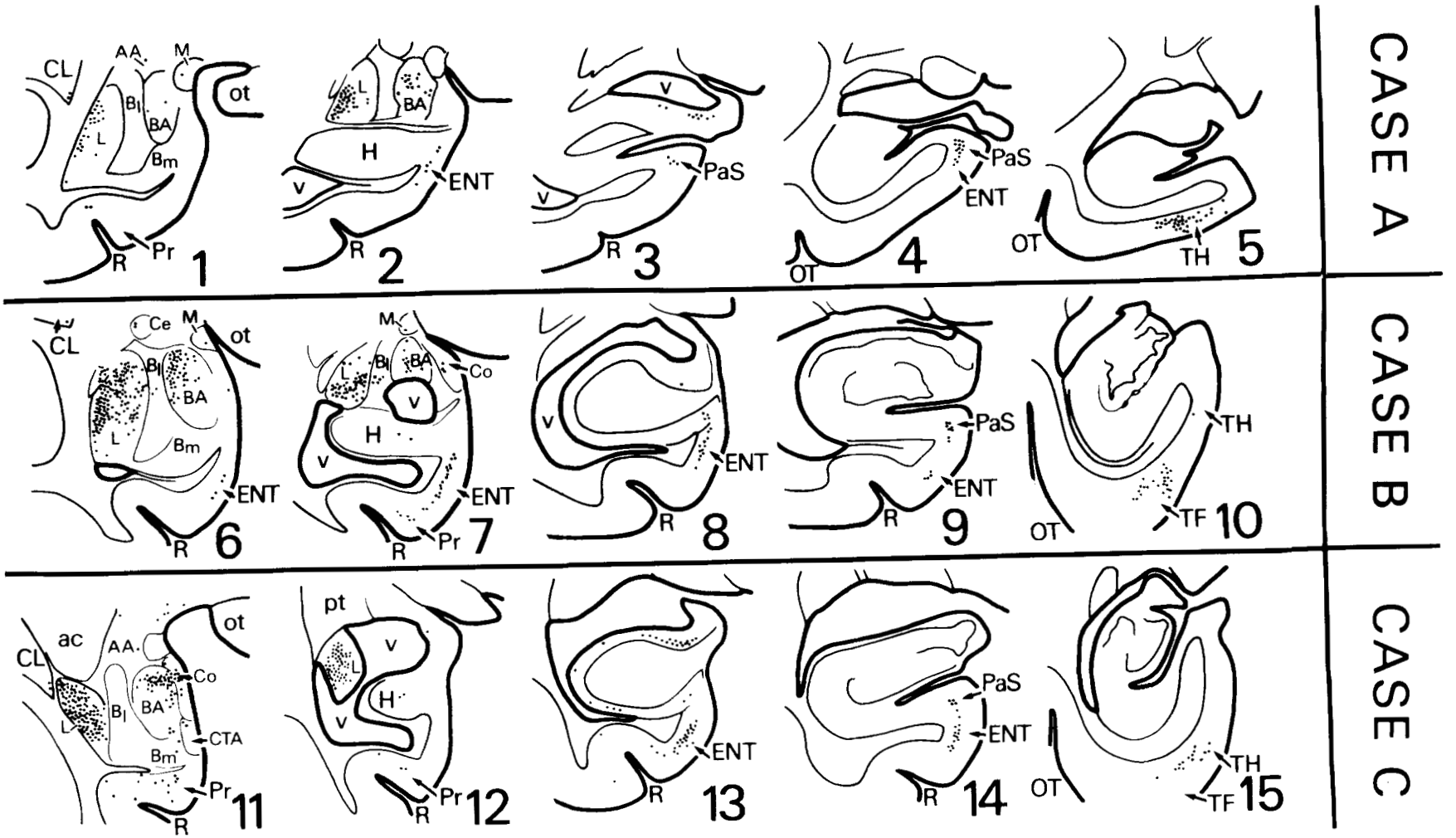

Fig. 6. Neuronal labeling found along the parahippocampal cortices, in the uncal region and in the amygdala. Retrograde labeling in the amygdala was less abundant in case A (injection site centered in TPg) than in cases B and C (injection centered in TPdg and TPa-p).

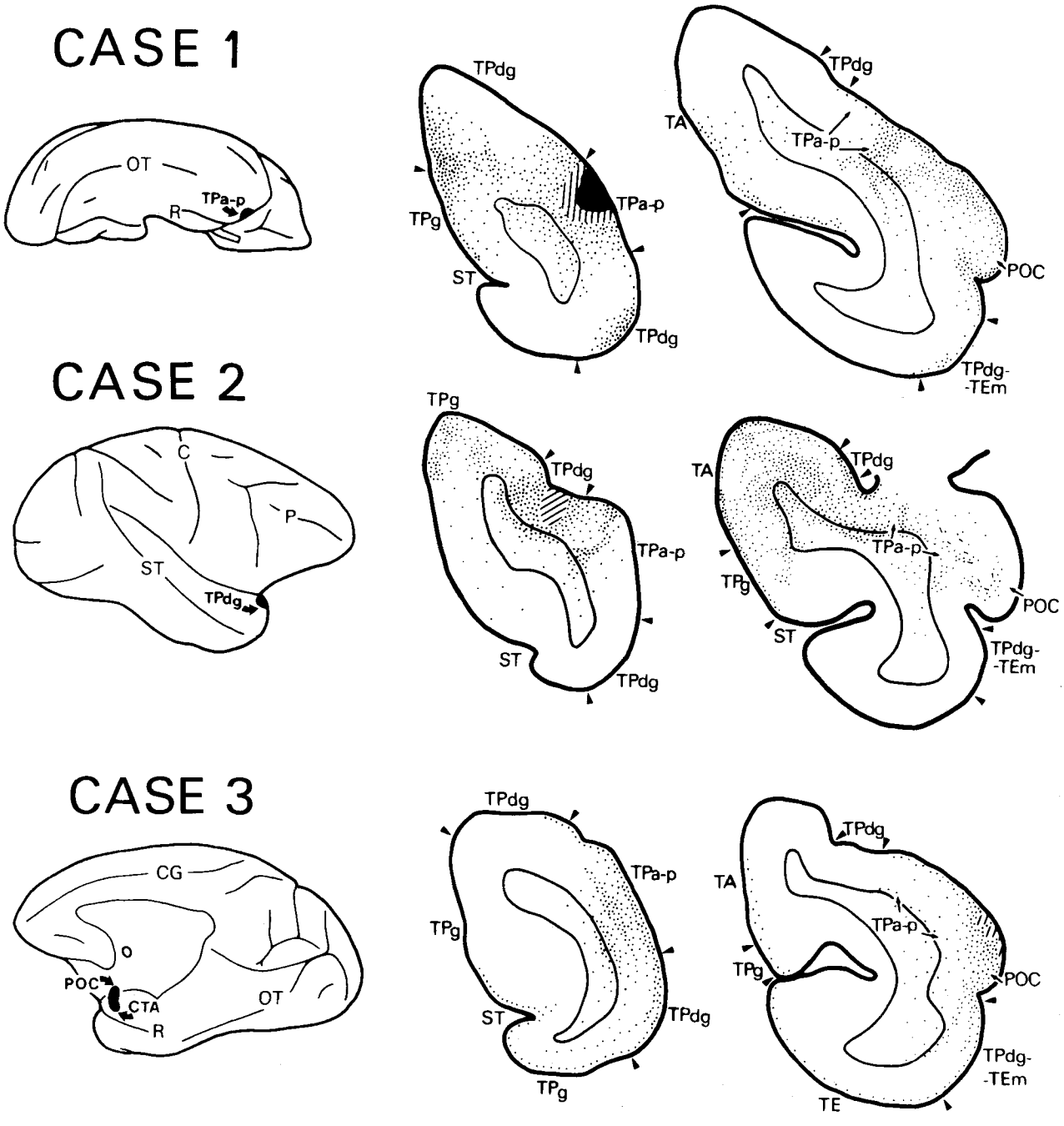

Fig. 7. TAA injection sites and labeling in TP in cases 1–3. The injection sites are shown as solid black, the halo as parallel lines, the labeled grains as black dots, and the labeled fibers as short black lines. Architectonic boundaries are indicated by arrowheads.

gion (areas 10–13 of Walker, '40; and OFg, OFdg, and OFap of Mesulam and Mufson, '82a) (Figs. 3–5). The medial aspect of the frontal lobe contained heavy labeling in all three cases. Medial frontal labeling included two major foci: (1) the medial aspect of Walker's area 10 (e.g., Fig. 3, sections 1,2) and (2) the subcallosal and parolfactory (PO) regions corresponding (in part) to area FL of von Bonin and Bailey '47 and areas 24 and 25 of Walker '40 (see Fig. 3, sections 5–7; Fig. 4, sections 5, 6; and Fig. 5, sections 4,5). Cases A and C also contained sparse labeling in the lateral aspect of area 10 (rostral tip of principalis cortex).

In case C, a few HRP-positive neurons were seen in the supracallosal portion of the anterior cingulate gyrus (Walker's area 24) (Fig. 5, sections 3,5).

Insula. No labeled neurons were seen in any sector of the insula in case A. In cases B and C, a small number of

positive perikarya were found in the agranular and dysgranular sectors of the insula (Fig. 4, sections 9,10,12: Fig. 5, sections 9–12).

Piriform olfactory cortex. All three cases had piriform olfactory cortex (POC) labeling but this was heaviest in cases B and C (Fig. 3, section 9; Fig. 4, section 9; Fig. 5, section 8).

Hypothalamus, claustrum, septum, and nucleus basalis. Positive neurons were found in the lateral, medial, and posterior hypothalamus of each case. All cases also contained labeled neurons in the ventral part of the claustrum. In cases B and C, labeled perikarya were found in the endopiriform nucleus (according to Krettek and Price, '78). Rare labeled neurons were observed in the septum. More pronounced labeling was seen in the nucleus basalis (NB). This labeling was present in all three cases, being heaviest in the posterior NBp (Ch4p) sector of Mesulam et al. ('83, '86).

Thalamus. In every case, HRP-filled neurons were seen in the posterior thalamus with the heaviest labeling in the medial pulvinar and the nucleus limitans (nomenclature according to Olszewski, '52) (Fig. 3, sections 13, 14; Fig. 4, section 14; Fig. 5, section 14). The anterior parvicellular medial geniculate nucleus was heavily labeled in cases A and B but to a much lesser extent in case C. Fewer labeled perikarya were also found in the suprageniculate nucleus, the magnocellular medial geniculate nucleus, the densocellular region of the medial dorsal nucleus, midline nuclei (e.g., the nucleus reuniens, the paraventricular nucleus, and the nucleus centralis densocellularis), the parafascicular nucleus, and the anterior tegmental nucleus. In cases B and C, a few positive neurons were found in the anterior medial nucleus. In general, the labeling of midline nuclei tended to be heavier in cases B and C.

Numerical analysis of labeled perikarya

The total numbers of labeled cortical (including POC and hippocampus) and amygdaloid neurons were quite comparable in cases A–C. These numbers were 3,443 in case A, 3,822 in case B, and 3,373 in case C. However, the distribution of these neurons showed differences. For example, in case A, which had the dorsal HRP injection site, 33% of all retrogradely labeled neurons were situated in auditory association cortex of the superior temporal gyrus. This percentage was 6% and 13% for cases B and C, respectively. Visual association input from inferotemporal cortex, was substantial (9%) only in case C with the ventral TP injection site, whereas this proportion was no more than 1% in the other two cases. Amygdaloid and olfactory input also showed consistent differences. Thus, 18% and 13% of all labeled cortical and amygdaloid neurons in cases C and B were located in the amygdala whereas this percentage fell to 5% in case A. Although labeled POC neurons never constituted more than 1% of the total retrograde labeling, they were more numerous in cases B and C.

In each of the three HRP cases, virtually all of the positive labeled perikarya were found in layers 3, 5, and 6. The proportion of labeled neurons located in the supra- and infragranular layers varied from region to region in a pattern that was consistent in all the cases. Thus, neurons that projected to TP from isocortical association areas (e.g., areas TA, TE, prefrontal cortex) were more heavily concentrated within supragranular layers whereas the projections from nonisocortical paralimbic areas (e.g., OFdg, entorhinal) tended to arise predominantely from deeper layers of cortex.

TAA injections

In order to obtain further evidence for the projections demonstrated with the HRP injections, 11 additional animals were examined, each with a TAA injection in one of the areas that contained retrogradely labeled neurons. These 11 TAA injections fall into five groups:

Intrinsic TP injections. In cases 1 and 2, TAA was injected within TP (Fig. 7). In case 1, the injection was in TPa-p, with a minimal extension into anterior dorsal TPdg. Moderate to heavy labeling was seen in layer 1 of TPg, TA, and the upper bank of the superior temporal sulcus, as well as in ventral TPdg, TPa-p, and POC. In case 2, the TAA injection was restricted to anterior dorsal TPdg. Anterograde labeling was found in all cortical layers in dorsal TPdg, TPg, and TA. Moderate labeling was also seen in TPa-p and POC. Both cases 1 and 2 confirm the intrinsic connections described in the HRP cases.

Limbic injections. In case 3, TAA was injected into CTA with spread to POC (Fig. 7). Moderate to heavy anterograde labeling was seen in POC and TPa-p with light label in ventral TPdg. Labeling was also found in layer 1 of TPg, TE, and lateral TA. In case 4, the injection site was centered within the lateral entorhinal area 28b, at the level of the anterior uncus (Fig. 8). The anterograde labeling found in this case was restricted to POC, TPa-p, and ventral TPdg. In case 5, TAA was injected into an anterior sector of medial entorhinal area 28a with minor spread to the surrounding area 28i. In this case, a heavy projection was seen in POC and in ventral TPg (Fig. 8). Additional labeling was also found in TPa-p, TPdg, and dorsal TPg. These results are in agreement with those of the HRP cases, since case A showed entorhinal labeling restricted to medial area 28a (Fig. 3, section 10; (Fig. 6, section 4), whereas HRP retrograde labeling was also found in 28i and 28b in cases B and C (Fig. 4, sections 11,12; Fig. 5, section 13; Fig. 6, sections 9,13,14). Furthermore, these cases indicate that efferents from medial temporal limbic areas to temporopolar cortex are directed mostly to the nonisocortical TPa-p and TPdg sectors.

Superior temporal injections. In case 6, an injection of TAA was restricted to PI (Fig. 8). Light to moderate labeling was found in dorsal TPdg and in TA. In case 7, TAA was injected into an anterior sector of area TA (Fig. 8). In this case, dense anterograde labeling was seen in dorsal TPg, TA, and anterior dorsal TPdg. The injections in both of these cases are within areas that are considered auditory association areas. The results of both cases 6 and 7 are consistent with the HRP cases and show that input from auditory areas is preferentially directed to the dorsal aspect of the temporal pole. Furthermore, these cases also show that the projection from the isocortical TA region is distributed mostly to the isocortical TPg sector, whereas the dysgranular PI area projects to TPdg more than to TPg.

Inferotemporal injections. In case 8, TAA was injected into the junction area between TEm and area TH (Fig. 9). Light to moderate labeling was found in TPa-p, POC, ventral TPdg, TEm, and TPg. An injection of TAA in case 9 was concentrated in the junction between TH and TF (Fig. 9). In this case, widespread projections were seen in ventral and intermediate TPg as well as in TPa-p. Area TEm is a visual association region. Areas TH and TF also have substantial visual input but may also have polysensory properties (Seltzer and Pandya, '76). Both cases 8 and 9 are concordant with the light but consistent projections from these areas to TP shown with HRP (Figs. 3–6). Area TEm

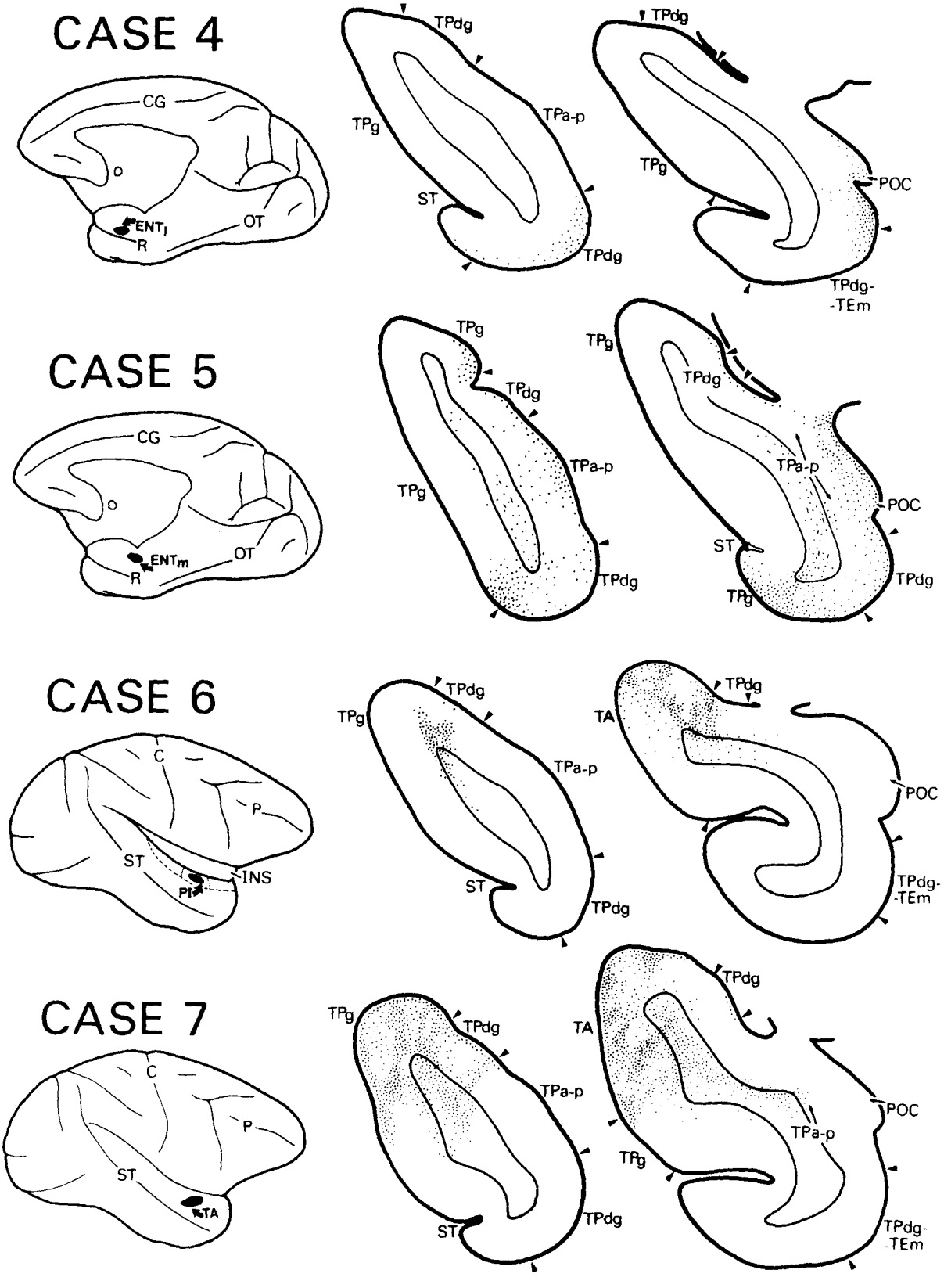

Fig. 8. TAA injection sites and labeling in TP in cases 4–7. The injection sites are shown as solid black, the labeled grains as black dots, and the labeled fibers as short black lines. Architectonic boundaries are indicated by arrowheads. In case 6, the lateral (sylvian) fissure has been opened to show the insula and the adjacent parainsular area.

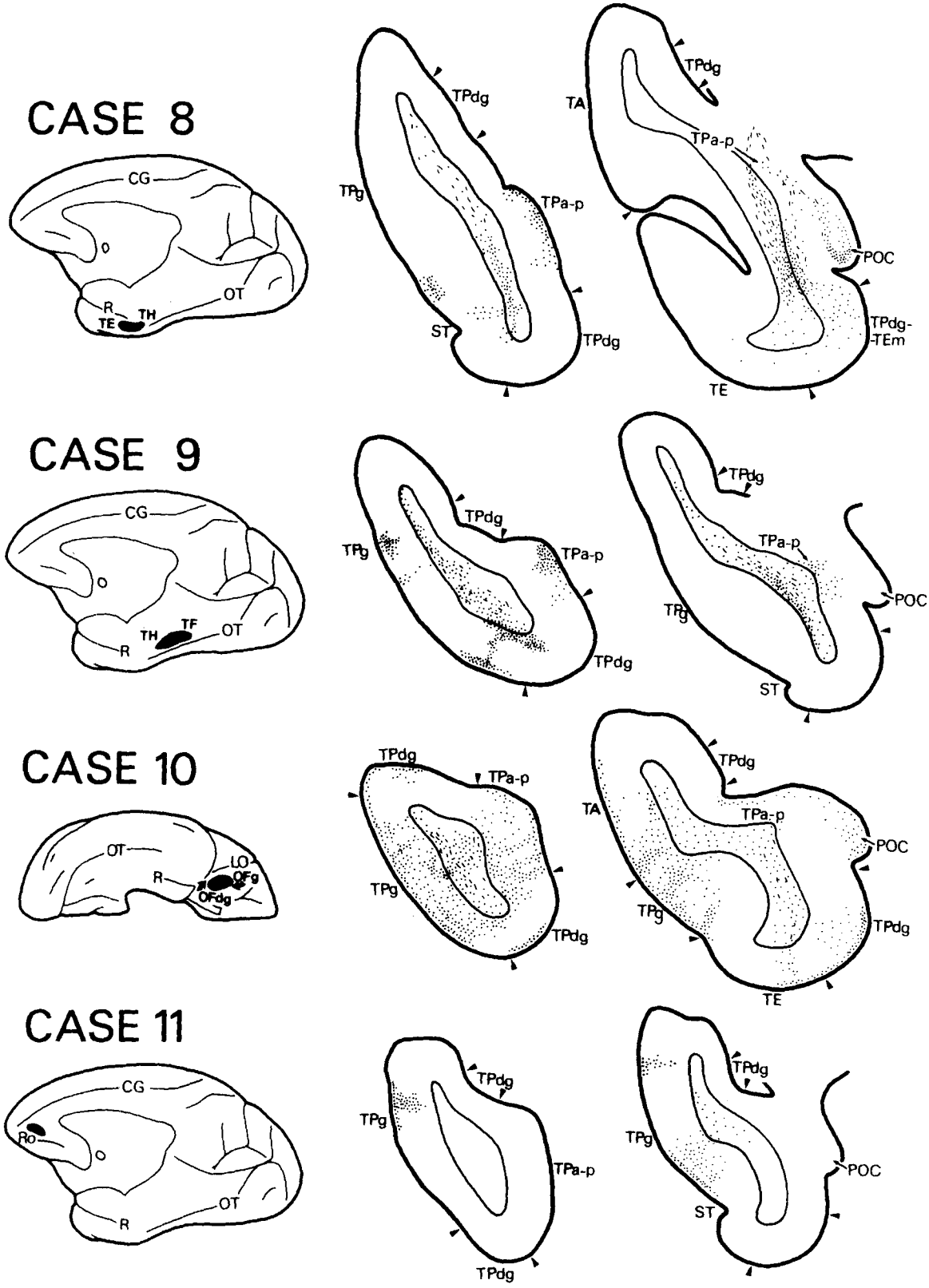

Fig. 9. TAA injection sites and labeling in TP cases 8–11. The injection sites are shown as solid black, the labeled grains as black dots, and the labeled fibers as short black lines. Architectonic boundaries are indicated by arrowheads.

projects almost exclusively to the medial and ventral parts of TP, whereas TH-TF projects more substantially to the lateral TPg.

Frontal cortex injections. In case 10, the TAA injection site extended from the granular sector of the orbitofrontal area 13 (OFg) to the caudal dysgranular sector (OFdg) in areas 12 and 13 (Fig. 9). In this case the anterograde labeling was widely distributed in all regions of TP. A heavy concentration of label filled layer 1 throughout almost all of the anterior portion of TP. Heavy labeling was also concentrated in layer 3 and formed radial columns in TPg, in TPa-p, and in TE. Labeling was also seen in POC. In case 11, a small injection of TAA was located in granular frontal area 10 of Walker. Moderate labeling seen in this case was restricted mainly to TPg. Both cases 10 and 11, with frontal projections into TP, confirm the observations based on the HRP injections. They also provide further support for the hypothesis that projections from granular, isocortical regions (as in case 11) are preferentially directed to the isocortical parts of TP.

DISCUSSION

In keeping with the other paralimbic areas, the temporopolar (TP) region provides an architectonic transition from the olfactory allocortex (POC) to the lateral temporal association areas (Gower, '81; Gower and Mesulam, '82; Mesulam and Mufson, '82a). The agranular periallocortical sector (TPa-p) is surrounded by a dysgranular zone (TPdg) that is, in turn, flanked by granular cortex (TPg). Dorsally, the cortical transition in TP proceeds toward the auditory association cortex of the anterior superior temporal gyrus. Ventrally, a similar transition proceeds toward the granular cortex of the inferotemporal visual association areas. The two lines of differentiation converge within the multimodal association cortex of the superior temporal sulcus.

The vast majority of the cortical neurons that project to TP are localized in three regions of the brain: the anterior temporal lobe, the orbitofrontal cortex, and the medial frontal region. The areas that provide these inputs can be subdivided into four major groups: (1) frontal and temporal heteromodal association cortex, (2) components of modality-specific auditory (anterior TA) and visual association (medial TE) areas, (3) paralimbic areas of the orbitofrontal, parolfactory, insular, and parahippocampal regions, and (4) limbic structures such as the amygdala, hippocampus, and POC. Additional inputs from hypothalamus, thalamus, claustrum and nucleus basalis are also present. This highly heterogeneous pattern of connectivity is consistent with the afferents of other paralimbic areas such as the insula (Mesulam and Mufson, '82b).

In a general sense, there seems to be a correspondence between the cytoarchitectonic nature of the TP subsector and the type of projections that it receives. For example, the more differentiated granular part of TP (TPg) receives a larger proportion of its afferents from parts of cortex that also have differentiated isocortical architecture. In contrast, the less-differentiated TPdg and TPa-p areas receive a larger proportion of their afferents from nonisocortical paralimbic regions and from limbic structures. An analogous correspondence has been demonstrated in the insula (Mesulam and Mufson, '82b).

There is also a topographical gradient in connectivity so that dorsal regions in TP are more closely related to the auditory modality whereas visual association inputs project mainly to the ventral sectors of TP. In fact, dorsal regions of TPg (as shown by case A) may receive close to 30% of all their cortical afferents from unimodal auditory association cortex. This strong auditory affiliation of dorsal TPg is analogous to the strong somatosensory affiliations of the granular insula (Ig) (Mesulam and Mufson, '85). Inputs from piriform olfactory cortex are primarily directed to the nonisocortical medial sectors of TP. Thus, the mediodorsal parts of TP provide a site for the potential convergence of olfactory and auditory impulses whereas the convergence of olfactory and visual inputs may occur in medioventral TP (Fig. 10).

Temporopolar cortex receives direct input from both the amygdala and the hippocampus. The amygdaloid afferents of TP are directed predominantely to the nonisocortical TPa-p and TPdg sectors. The hippocampal formation has relatively few cortical efferents, mostly restricted to paralimbic areas (Rosene and Van Hoesen, '77). Our observations indicate that TP should be added to this short list of cortical regions that receive hippocampal projections. Area FL and entorhinal cortex, two other regions with a relatively limited range of cortical connectivity, also have prominent connections with subsectors of TP.

Paralimbic areas play a crucial role in the establishment of sensory-limbic interactions. The projection patterns of TP clearly show that such interactions are also likely to take place in all subsectors of the temporal pole. Lesions including temporopolar cortex can give rise to the components of the Kluver-Bucy Syndrome (Akert et al., '61) and to a disruption of conspecific affiliative behaviors (Kling and Steklis, '76). These two types of behavioral deficits may reflect the breakdown of sensory limbic integration that follows temporopolar damage. Stimulation of the temporal pole results in profound alterations in heart rate, blood pressure, and respiration (Kaada et al., '49). These autonomic responses are probably mediated through the connections of TP with the amygdala (Herzog and Van Hoesen, '76). Lesions of the temporal pole can also lead to alterations in taste preferences (Bagshaw and Pribram, '53). Gustatory afferents from the insula and olfactory inputs from POC are likely to underlie the role of temporopolar cortex in alimentary behaviors.

The TP afferents originating in nonisocortical areas tend to come from cell bodies located in the deeper layers of cortex whereas those originating in the isocortical parts of cortex tend to come from neurons located in the more superficial layers of cortex. An identical pattern was also described in the afferent connections of insular cortex (Mufson and Mesulam, '82).

With respect to thalamic connectivity, our observations confirm earlier ones indicating that the major thalamic inputs of TP originate from the medial pulvinar, the nucleus limitans, and the medial geniculate nucleus (Gower, '81; Gower and Mesulam, '82). Additional intralaminar and midline nuclei also project to TP, especially to its nonisocortical sectors. The substantial projection from the medial pulvinar nucleus is consistent with prior observations showing that this nucleus has major connections with all paralimbic areas of the brain (Gower and Mesulam, '82; Mufson and Mesulam, '84).

Our observations on the connectivity of the temporal pole are in good agreement with the recent comprehensive study of Markowitsch et al. ('85). The availability of medially situated injection sites in our experiments provide additional information on the limbic connectivity of this region.

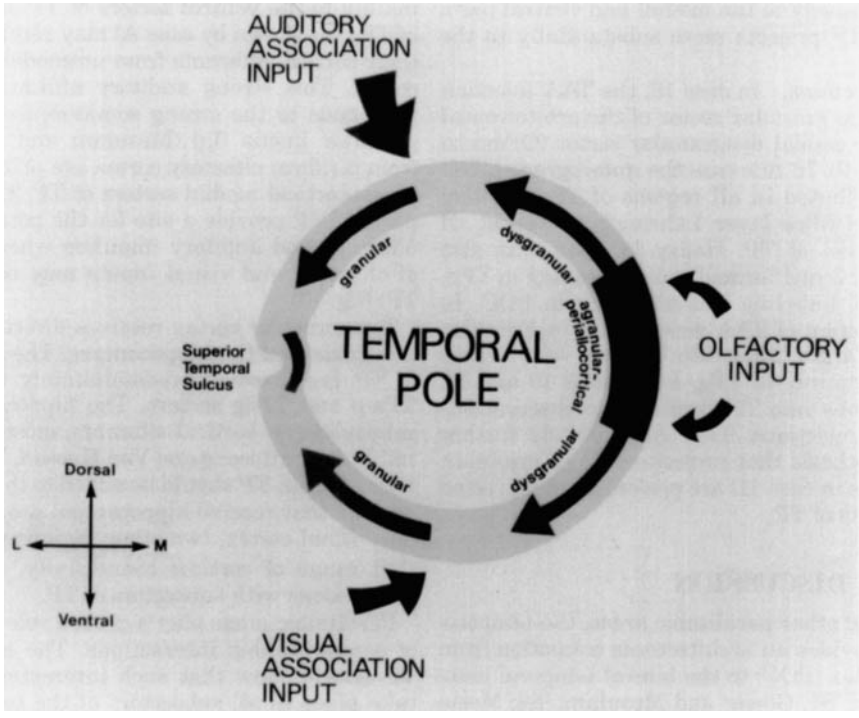

Fig. 10. Schematic diagram showing the modality-specific afferent inputs to the architectonic subsectors of the temporal pole.

ACKNOWLEDGMENTS

We wish to thank Leah Christie, Terry Martin, and Richard Plourde for expert secretarial, histological and photographic assistance. We are also grateful to Dr. Galaburda for providing some of the material for architectonic analysis. This work was supported in part by the Fogarty Fellowship, FO5 TWO3624, the U.S.-Spanish Joint Committee grant TPB 8402034, the Javits Neuroscience Investigator Award, the McKnight Foundation, and an Alzheimer's Research Center NIA AG-05134.

LITERATURE CITED

Akert, K., R.A. Gruesen, C.N. Woolsey, and D.R. Meyer (1961) Kluver-Bucy syndrome in monkeys with neocortical ablations of temporal lobe. Brain *84:*480–498.

Amaral, D.G., and J.L. Price (1984) Amygdalo-cortical projections in the monkey (Macaca fascicularis). J. Comp. Neurol. *230:*465–496.

Bagshaw, M.H., and K.H. Pribram (1953) Cortical organization in gustation (Macaca mulatta). J. Neurophysiol. *16:*499–508.

Bonin, G.V., and P. Bailey (1947) the Neocortex of Macaca mulatta. Urbana: University of Illinois Press.

Brodmann, K. (1909) Vergleichende Lokalisationslehre der Grosshirnrinde. Leipzig: J.A. Barth.

Cowan, W.M., D.I. Gottlieb, A.E. Hendrickson, J.L. Price, and T.A. Woolsey (1972) The autoradiographic demonstration of axonal connections in the central nervous system. Brain Res. *37:*21–51.

Galaburda, A.M., and D.N. Pandya (1983) The intrinsic architectonic and connectional organization of the superior temporal region of the rhesus monkey. J. Comp. Neurol. *221:*169–184.

Gower, E.C. (1981) Architecture and Thalamic Connections of Macaque Temporal Polar Cortex. Doctoral Thesis: Massachusetts Institute of Technology.

Gower, E.C., and M.-M. Mesulam (1982) Cytoarchitecture correlated with distribution of AChE in monkey temporopolar cortex. Anat. Rec. *202:*67A–68A (abstract).

Herzog, A.G., and G.W. Van Hoesen (1976) Temporal neocortical afferent connections to the amygdala in the rhesus monkey. Brain Res. *115:*57–69.

Jones, E.G., and T.P.S. Powell (1970) An anatomical study of converging sensory pathways within the cerebral cortex of the rhesus monkey. Brain *93:*793–820.

Kaada, B.R., K.H. Pribram, and J.A. Epstein (1949) Respiratory and vascular responses in monkeys from temporal pole, insula, orbital surface and cingulate gyrus. J. Neurophysiol. *12:*348–356.

Kling, A., and H.D. Steklis (1976) A neural substrate for affiliative behavior in nonhuman primates. Brain Behav. Evol. *13:*216–238.

Kosel, K.C., G.W. Van Hoesen, and D.L. Rosene (1982) Non-hippocampal cortical projections from the entorhinal cortex in the rat and rhesus monkey. Brain Res. *244:*201–213.

Krettek, J.E., and J.C. Price (1978) A description of the amygdaloid complex in rat and cat, with observations on intra-amygdaloid axonal connections. J. Comp. Neurol. *178:*255–280.

Lauer, E.W. (1945) The nuclear pattern and fiber connections of certain basal telencephalic centers in the macaque. J. Comp. Neurol. *82:*215–254.

Lorente de Nó, R. (1933) Studies on the structure of the cerebral cortex. I. The area entorhinalis. J. Psychol. Neurol. *45:*381–438.

Markowitsch, H.J., D. Emmans, E. Irle, M. Streicher, and B. Preilowski (1985) Cortical and subcortical afferent connections of the primate's temporal pole: A study of rhesus monkeys, squirrel monkeys, and marmosets. J. Comp. Neurol. *242:*425–458.

Mesulam, M.-M. (1978) Tetramethyl benzidine for horseradish peroxidase neurohistochemistry: A non-carcinogenic blue reaction-product with superior sensitivity for visualizing neural afferents and efferents. J. Histochem. Cytochem. *26:*106–117.

Mesulam, M.-M. (1982) Principles of horseradish peroxidase neurohistochemistry and their applications for tracing neural pathways-axonal transport, enzyme histochemistry and light microscopic analysis. In M.-M. Mesulam (ed): Tracing Neural Connections with Horseradish Peroxidase. Chichester: John Wiley and Co., pp. 1–151.

Mesulam, M.-M., E. Hegarty, H. Barbas, K.A. Carson, E.C. Gower, A.G. Knapp, M.B. Moss, and E.J. Mufson (1980) Additional factors influencing sensitivity in the tetramethyl benzidine method for horseradish peroxidase neurohistochemistry. J. Histochem. Cytochem. *28:*1255–1259.

Mesulam, M.-M., and E.J. Mufson (1982a) Insula of the old world monkey: I: Architectonics in the insulo-orbito-temporal component of the paralimbic brain. J. Comp. Neurol. *212:*1–22.

Mesulam, M.-M., and E.J. Mufson (1982b) Insula of the old world monkey: III: Efferent cortical output and comments on function. J. Comp. Neurol. *212:*38–52.

Mesulam, M.-M., and E.J. Mufson (1984) Neural inputs into the nucleus basalis of the substantia innominata (Ch4) in the rhesus monkey. Brain *107:*253–274.

Mesulam, M.-M., and E.J. Mufson (1985) The insula of Reil in man and monkey. In E.G. Jones and A.A. Peters (eds): Cerebral Cortex, Vol. 4. New York: Plenum Press, pp. 179–226.

Mesulam, M.-M., E. J. Mufson, A.I. Levey, and B.H. Wainer (1983) Cholinergic innervation of cortex by the basal forebrain: Cytochemistry and cortical connections of the septal area, diagonal band nuclei, nucleus basalis (substantia innominata) and hypothalamus in the rhesus monkey. J. Comp. Neurol. *214:*170–197.

Mesulam, M.-M., E.J. Mufson, and B.H. Wainer (1986) Three-dimensional representation and cortical projection topography of the nucleus basalis (Ch4) in the macaque: Concurrent demonstration of choline acetyltransferase and retrograde transport with a stabilized tetramethylbenzidine method for HRP. Brain Res. *367:*301–308.

Mufson, E.J., and M.-M. Mesulam (1982) Insula of the old world monkey. II: Afferent cortical input and comments on the claustrum. J. Comp. Neurol. *212:*23–37.

Mufson, E.J., and M.-M. Mesulam (1984) Thalamic connections of the insula in the rhesus monkey and comments on the paralimbic connectivity of the medial pulvinar nucleus. J. Comp. Neurol. *227:*109–120.

Olszewski, J. (1952) The Thalamus of the Macaca Mulatta. Basel: S. Karger.

Pandya, D.N., and H.G.J.M. Kuypers (1969) Cortico-cortical connections in the rhesus monkey. Brain Res. *13:*13–36.

Pandya, D.N., and F. Sanides (1973) Architectonic parcellation of the temporal operculum in rhesus monkey and its projection pattern. Z. Anat. Entwickl. - Gesch. *139:*127–161.

Pribram, K.H., M.A. Lennox, and R.H. Dunsmore (1950) Some connections of the orbito-fronto-temporal, limbic and hippocampal areas of macaca mulatta. J. Neurophysiol. *13:*127–135.

Pribram, K.H., and P.D. MacLean (1953) Neuronographic analysis of medial and basal cerebral cortex. II. Monkey. J. Neurophysiol. *16:*324–340.

Ramón y Cajal, (1955) Studies on the Cerebral Cortex. Chicago: Yearbook, pp. 1–174.

Rosene, D.L., and M.-M. Mesulam (1978) Fixation variables in horseradish peroxidase neurohistochemistry. I. The effects of fixation time and perfusion procedure upon activity. J. Histochem. Cytochem. *26:*28–39.

Rosene, D.L., and G.W. Van Hoesen (1977) Hippocampal efferents reach widespread areas of cerebral cortex and amygdala in the rhesus monkey. Science *198:*315–317.

Seltzer, B., and D.N. Pandya (1976) Some projections to the parahippocampal area in the rhesus monkey. Exp. Neurol. *50:*146–160.

Seltzer, B., and D.N. Pandya (1978) Afferent cortical connections and architectonics of the superior temporal sulcus and surrounding cortex in the rhesus monkey. Brain Res. *149:*1–24.

Turner, B.H., M. Mishkin, and M. Knapp (1980) Organization of the amygdalopetal projections from modality-specific cortical association areas in the monkey. J. Comp. Neurol. *191:*515–543.

Van Hoesen, G.W., M.-M. Mesulam, and R. Haaxma (1976) Temporal cortical projections to the olfactory tubercle in the rhesus monkey. Brain Res. *109:*375–381.

Van Hoesen, G.W., D.N. Pandya, and N. Butters (1972) Cortical afferents to the entorhinal cortex of the rhesus monkey. Science *175:*1471–1473.

Van Hoesen, G.W., and D.N. Pandya (1975a) Some connections of the entorhinal (area 28) and perirhinal (area 35) cortices of the rhesus monkey. I. Temporal lobe afferents. Brain Res. *95:*1–24.

Van Hoesen, G.W., and D.N. Pandya (1975b) Some connections of the entorhinal (area 28) and perirhinal (area 35) cortices of the rhesus monkey. III. Efferent connections. Brain Res. *95:*39–59.

Van Hoesen, G.W., D.L. Rosene, and M.-M. Mesulam (1979) Subicular input from temporal cortex in the rhesus monkey. Science *205:*608–610.

Van Hoesen, G.W., E.H. Yeterian, and R. Lavizzo-Mourey (1981) Widespread corticostriate projections from temporal cortex of the rhesus monkey. J. Comp. Neurol. *199:*205–219.

Walker, A.E. (1940) A cytoarchitectural study of the prefrontal area of the macaque monkey. J. Comp. Neurol. *73:*59–86.